

*CH<sub>4</sub> uptake along a successional gradient  
in temperate alpine soils*

**Cole G. Brachmann, Guillermo  
Hernandez-Ramirez & David S. Hik**

**Biogeochemistry**  
An International Journal

ISSN 0168-2563  
Volume 147  
Number 2

Biogeochemistry (2020) 147:109-123  
DOI 10.1007/s10533-019-00630-0

**Your article is protected by copyright and all rights are held exclusively by Springer Nature Switzerland AG. This e-offprint is for personal use only and shall not be self-archived in electronic repositories. If you wish to self-archive your article, please use the accepted manuscript version for posting on your own website. You may further deposit the accepted manuscript version in any repository, provided it is only made publicly available 12 months after official publication or later and provided acknowledgement is given to the original source of publication and a link is inserted to the published article on Springer's website. The link must be accompanied by the following text: "The final publication is available at [link.springer.com](http://link.springer.com)".**



# CH<sub>4</sub> uptake along a successional gradient in temperate alpine soils

Cole G. Brachmann · Guillermo Hernandez-Ramirez · David S. Hik

Received: 25 March 2019 / Revised: 6 December 2019 / Accepted: 9 December 2019 / Published online: 7 January 2020  
© Springer Nature Switzerland AG 2020

**Abstract** The effects of climate change appear to be amplified in mountains compared with lowland areas, with rapid changes in plant community composition, soil properties, and increased substrate for biological development following retreat of glaciers. Associated soil gaseous fluxes in alpine ecosystems contribute to the global balance of greenhouse gases, but methane and carbon dioxide soil fluxes and their controls are not well known. We used a dynamic closed-chamber method to measure methane and carbon dioxide fluxes

along a successional gradient during the peak growing season in the North Selkirk Mountains, British Columbia, Canada. Soil physico-chemical properties, vegetation cover, and topographic variables were quantified to determine mechanisms influencing these fluxes. Mean methane uptake ranged from  $-155 \mu\text{g CH}_4\text{-C m}^{-2} \text{ h}^{-1}$  in well vegetated sites to zero in recently deglaciated terrain. Soil total carbon (TC) and water content were the primary drivers of methane uptake. Sites with TC greater than 4% and moisture below 0.22 water fraction by volume (w.f.v) corresponded to the strongest methane sinks. Increased vegetation cover and relatively drier soil conditions, anticipated with future climate change, suggest that methane uptake may increase in these alpine ecosystems.

Responsible Editor: James Sickman

**Electronic supplementary material** The online version of this article (<https://doi.org/10.1007/s10533-019-00630-0>) contains supplementary material, which is available to authorized users.

C. G. Brachmann (✉) · D. S. Hik  
Department of Biological Sciences, University of Alberta,  
Edmonton, Canada  
e-mail: cbrachma@ualberta.ca

*Present Address:*

C. G. Brachmann  
Department of Earth Sciences, University of Gothenburg,  
Gothenburg, Sweden

G. Hernandez-Ramirez  
Department of Renewable Resources, University of  
Alberta, Edmonton, Canada

D. S. Hik  
Department of Biological Sciences, Simon Fraser  
University, Burnaby, Canada

**Keywords** Columbia mountains · Methane · Soil fluxes · Alpine · Deglaciated terrain

## Introduction

In most parts of the world mountains are warming at an accelerated rate compared to lowland areas, a process termed elevation dependent warming (Pepin et al. 2015; IPCC 2019). CH<sub>4</sub> and CO<sub>2</sub> are biogenic greenhouse gases with large terrestrial pools that are dynamically exchanged with the atmosphere, but

the direction and magnitude of these fluxes are still largely unknown in temperate alpine regions, including western North America (Oertel et al. 2016). The balance between emissions and uptake from mountain soils vary with environmental conditions and improved estimates will contribute to the development of better constrained global and regionally sensitive climate models (Nisbet et al. 2009).

Soil fluxes include the net uptake or release of a gas between the soil and the atmosphere. These gas exchanges are controlled by both the microbial and physical aspects of the soil (Smith et al. 2003). Microbes are responsible for the production or consumption of different gaseous products that subsequently diffuse into or out of the soil depending primarily on concentration gradients. However, the rate of diffusion is controlled by the pore size, aggregate size, and amount of water filled pore space in the soil (Smith et al. 2003; Venterea and Baker 2008). In this way soil fluxes result from a combination of the microbial processing and physical movement of gas in soil.

While mountains cover about 25% of the Earth's terrestrial surface, only about 3% is classified as alpine biome (Hu and Bliss 2018). Alpine communities are heterogeneous in terms of topography, vegetation, and edaphic properties. An examination of the mechanisms influencing CH<sub>4</sub> and CO<sub>2</sub> fluxes in the alpine requires consideration of differences in the type of soil, vegetation cover, elevation, and time since deglaciation across natural spatial gradients. Recently deglaciated Regosolic soils are formed following progressive glacial recession leading to newly exposed terrain (Chersich et al. 2015; IPCC 2019). These recently deglaciated areas represent the initial baseline for CH<sub>4</sub> and CO<sub>2</sub> fluxes since vegetation and microbial communities are poorly developed. Established alpine tundra has comparatively more developed soils, often Brunisols, and the vegetation is dominated by graminoid and ericaceous species. Along an elevational gradient, the alpine zone slopes through the subalpine ecotone towards montane forest, which have different soil characteristics due to time since deglaciation and vegetation succession. In many regions the montane forest treeline is advancing upslope or becoming more heavily vegetated as tree density increases (Cannone and Pignatti 2014; Camarero et al. 2017).

Most studies of CH<sub>4</sub> and CO<sub>2</sub> fluxes in temperate alpine ecosystems have been conducted in China (Wei et al. 2015; Zhu et al. 2015; Wu et al. 2017; Fu et al. 2018), Europe (Kitzler et al. 2006; Koch et al. 2007; Chiri et al. 2015, 2017; Hofmann et al. 2016a; Mutschlechner et al. 2018), and Colorado (Brooks et al. 1997; Knowles et al. 2015; Lin et al. 2017). To expand on this geographic coverage, we measured alpine soil CH<sub>4</sub> and CO<sub>2</sub> fluxes in the Columbia Mountains, British Columbia, Canada. Specifically, we compared fluxes of (1) recently deglaciated soils (RDG sites) with more developed alpine soils (Alpine sites), and (2) along a successional gradient characterized into three elevational bands (high, mid, and low) during the peak of the summer growing season. We simultaneously investigated the physical and chemical soil mechanisms controlling CH<sub>4</sub> and CO<sub>2</sub> fluxes including vegetation cover, soil moisture (as an inverse proxy for aeration), and temperature, as they have previously been identified as strong predictors (Borken et al. 2003; Parkin and Kaspar 2003; Oertel et al. 2016). Finally, we compared our methane fluxes with measurements from other biomes to assess the potential impact of alpine fluxes in a global context.

## Methods

### Site characteristics

The North Selkirk Mountains are located in the Columbia Mountains in southeastern British Columbia, Canada. Geologically these mountains are comprised of Proterozoic and Paleozoic North American rocks (Simony and Carr 2011). The highest peaks in our immediate study area were between 2515 and 3167 m above sea level, and numerous mountain glaciers persist above 2150 m. The higher elevation forests are dominated by subalpine fir (*Abies lasiocarpa*), and the entire region can be characterized as part of the Montane Cordillera Ecozone (<http://ecozones.ca/english/zone/index.html>). The upper limit of treeline is located around 2000 m, but with considerable variation depending on local conditions, including aspect, slope and local disturbance (Davis et al. 2018).

Our field measurements were conducted at the peak of the growing season in August 2017 in Bachelor Pass (51° 31' 21.06" N; 117° 57' 31.55" W), at several sites

**Table 1** Soil properties and vegetation cover for each field site in Bachelor Pass, British Columbia

Site	Soil order	pH	EC dS m <sup>-1</sup>	NO <sub>3</sub> mg N kg <sup>-1</sup>	NH <sub>4</sub> mg N kg <sup>-1</sup>	TN mg N mg <sup>-1</sup> %	TC mg C mg <sup>-1</sup> %
RDG	Regosol	9.3 ± 0.0	0.05 ± 0.00	0.5 ± 0.0	0.6 ± 0.1	0.00 ± 0.00	0.35 ± 0.02
Alpine	Brunisol	5.4 ± 0.2	0.02 ± 0.00	0.4 ± 0.0	2.8 ± 0.8	0.43 ± 0.06	8.20 ± 1.94
High	Brunisol	6.2 ± 0.5	0.03 ± 0.01	0.4 ± 0.0	1.3 ± 0.2	0.39 ± 0.25	3.26 ± 2.03
Mid	Brunisol	5.4 ± 0.1	0.02 ± 0.01	0.4 ± 0.1	2.5 ± 0.7	0.62 ± 0.12	5.47 ± 1.12
Low	Brunisol	5.3 ± 0.1	0.06 ± 0.01	0.6 ± 0.1	18.6 ± 1.8	1.58 ± 0.21	10.02 ± 2.11
Site	C:N	δ <sup>15</sup> N ‰	δ <sup>13</sup> C ‰	Soil temperature °C	Surface Temperature °C	Air Temperature °C	Volumetric water content w.f.v
RDG	NA	NA	- 5.4 ± 0.3	17.3 ± 0.7	16.2 ± 0.9	19.7 ± 1.0	0.05 ± 0.01
Alpine	16.86 ± 2.91	4.9 ± 0.3	- 24.0 ± 1.3	20.9 ± 0.6	28.9 ± 1.0	22.6 ± 0.8	0.27 ± 0.01
High	8.96 ± 0.45	4.8 ± 1.0	- 22.3 ± 1.9	24.2 ± 1.0	32.2 ± 1.5	24.4 ± 0.9	0.15 ± 0.02
Mid	8.89 ± 0.51	5.6 ± 0.7	- 24.4 ± 0.2	27.1 ± 0.8	45.2 ± 1.9	24.9 ± 0.5	0.21 ± 0.03
Low	6.95 ± 1.29	4.0 ± 0.1	- 27.3 ± 1.5	27.1 ± 0.5	40.3 ± 1.8	24.7 ± 0.4	0.53 ± 0.02
Site	% clay	% silt	% sand		% vegetation cover		
RDG	10 ± 0	33 ± 4	57 ± 4		2 ± 1		
Alpine	9 ± 2	45 ± 8	46 ± 7		92 ± 3		
High	8 ± 0	35 ± 3	57 ± 3		36 ± 14		
Mid	11 ± 1	45 ± 2	44 ± 2		88 ± 4		
Low	12 ± 1	46 ± 4	42 ± 4		85 ± 4		

Site refers to locations along the elevational transect (High, Mid, Low) and relative to terminus of the retreating Easy Glacier (Recently Deglaciated: RDG, and Alpine). Values are means ( $n = 10$  for RDG and Alpine,  $n = 6$  for Low and Mid, and  $n = 4$  for High, based on number of chambers installed) ± 1 standard error (SE)

along elevational and successional gradients. The first set of measurements allowed us to directly compare recently deglaciated terrain near the terminus of the Easy Glacier (RDG sites) with later successional terrain on the west side of Bachelor Pass (Alpine sites). Both the Alpine and RDG sites were located at the top of the mountain pass at around 2100 m. The second set of measurements were focused within “high” (2100 m), “mid” (2050 m), and “low” (2000 m) elevation sites along two successional transects located on the east side of the pass.

The recently deglaciated (RDG) sites were located within 50–80 m from the current glacier terminus and were likely exposed during the past decade (Brachmann 2019). They are characterized by grey silty Regosol soils with limited nutrient levels and vegetation cover (< 5%) (Table 1). Alpine sites had higher vegetation cover (> 80%), mostly graminoids and heather, and more developed Brunisol soils with higher nutrients, better defined horizons, and more

organic matter (Table 1). The successional transects had a variety of vegetation types and their soils were also classified as Brunisols, including low sites located below treeline.

#### Flux measurements

A dynamic closed-chamber method was used to measure the water vapour, CH<sub>4</sub> and CO<sub>2</sub> fluxes using PVC plastic chambers comprised of a base and a top. Each chamber top had a gasket and rubber band for sealing the top with the base, a vent tubing to equalize pressure to the atmosphere and reflective tape to reduce the effect of warming from sunlight. Five chamber bases were installed in each of two sub-plots in the RDG site, for a total of ten chamber bases in the RDG site. Ten chambers bases were also installed in the Alpine sites following the same arrangement as the RDG sites. Three chamber bases were installed in each

of three elevational bands (high, mid, low) in the first transect. For the second transect three chamber bases were installed in the low elevation band and four at the intermediate elevation band. The three chamber locations in the high elevation band from transect 1 were resampled with double frequency as two of the plastic bases failed during their installation in transect 2.

Surface flux measurements were conducted in situ during both morning and afternoon of three consecutive days using a portable laser analyzer (GasScouter G4301, Picarro Inc, Santa Clara, CA, USA) connected to plastic flux chambers for gas recirculation using Teflon 6.4 mm O.D. tubing. The laser analyzer recorded both the CO<sub>2</sub> and CH<sub>4</sub> mixing ratios in dry air in each chamber location. Chamber bases (8.3 cm height × 16 cm diameter) were installed roughly 5 cm deep in the soil one day prior to measurements and left for the duration of the field sampling protocol (Chikowo et al. 2004; Neu et al. 2011). Bases were either installed in areas naturally devoid of vegetation or aboveground vegetation was carefully removed by hand to determine the contribution of the soil itself to CH<sub>4</sub> and CO<sub>2</sub> fluxes, although soil crusts, cryptogams and some roots remained. Chamber tops (11.5 cm height × 16 cm diameter) were placed and sealed onto the bases when flux measurements were taken, each measurement interval was five minutes to allow for adequate mixing of gas at a flow rate of 0.87 standard L min<sup>-1</sup> and an accurate non-steady state flux to be recorded. Chamber tops were then flushed with ambient air for one minute afterward in preparation for the next flux measurement.

The laser analyzer records a measurement of gas concentration approximately every 1.25 s. Periods of a few seconds at the beginning and end of each five-minute measurement interval were discarded as they are associated with disturbance of the gas circulation flow and are not accurate representations of the flux of the focal gas species. Fluxes were calculated using ordinary least squared linear regressions of concentration measurements with time for both CH<sub>4</sub> and CO<sub>2</sub> based on the derived regression coefficients and the ideal gas law.

$$\text{Flux}_{\text{Gas}} = \frac{\left( \frac{[\text{Gas}]_{t2} - [\text{Gas}]_{t1}}{t2 - t1} \right) * P * V * 12.01 * 60}{(R * T_{\text{air}} * A)}$$

where Flux<sub>Gas</sub> = Linear flux of focal gas (CO<sub>2</sub> or CH<sub>4</sub>) in mg CO<sub>2</sub>-C m<sup>-2</sup> h<sup>-1</sup> or µg CH<sub>4</sub>-C m<sup>-2</sup> h<sup>-1</sup>; respectively. [Gas]<sub>t2</sub> = Concentration of gas at time 2. [Gas]<sub>t1</sub> = Concentration of gas at time 1. t<sub>2</sub> = time 2 in s. t<sub>1</sub> = time 1 in s. P = Air pressure in atm. V = Volume of the chamber in m<sup>3</sup>. R = Molar gas constant (0.082058 L atm mol<sup>-1</sup> k<sup>-1</sup>). T<sub>air</sub> = Air temperature in Kelvins. A = Area of chamber.

## Soils and environmental measurements

Soil temperature, volumetric water content, ground surface temperature, altitude, and ambient pressure were recorded in situ at each chamber location (n = 36). Soil temperature and volumetric water content were measured with a Steven's HydraProbe, surface temperature was measured with an Apogee MI-230 infrared radiometer, altitude and air pressure was measured using a Testo 511 handheld altimeter (Table 1). Composited soil samples (n = 36) were also collected from each chamber location and analyzed for the following properties: total nitrogen (TN), total carbon (TC), carbon: nitrogen ratio (C:N), δ<sup>15</sup>N, δ<sup>13</sup>C, NH<sub>4</sub><sup>+</sup>, NO<sub>3</sub><sup>-</sup>, pH, electrical conductivity (EC), and texture (Table 1). All soil samples were processed with a 2 mm sieve and the stored at the University of Alberta at 4 °C before analyses. All physico-chemical soil analyses were performed at the Natural Resources Analytics Laboratory (NRAL) at the University of Alberta.

The pH and EC were measured by mixing 10 g of each soil sample with 20 mL of water for a 2:1 water:soil ratio and determining the pH and EC of the resulting mixture with a calibrated Fisher AR 20 pH/EC meter. Available ammonium and nitrate were determined by a nutrient extraction with 50 mL of KCl mixed with 5 g of air-dried soil per sample and shaken for 30 minutes. The resulting mixtures were then filtered and NH<sub>4</sub><sup>+</sup> and NO<sub>3</sub><sup>-</sup> concentration was determined via colorimetric assay. TN, TC, and C:N ratio were measured using a Costech 4010 Elemental Analyzer following the dry combustion method.

Soil δ<sup>15</sup>N and δ<sup>13</sup>C were both measured by interfacing flash combustion method with isotopic ratio mass spectrometry. The N<sub>2</sub> or CO<sub>2</sub> gases resultant from the online combustion of the soil sample were run through a Thermo Finnigan Delta Advantage isotopic ratio mass spectrometer



(ThermoFisher Scientific, Waltham Massachusetts, USA). The IRMS determines the ratio of heavy:light isotope of the sample and compares it to the ratio of an international standard producing a delta value for the element. The  $\delta^{15}\text{N}$  and  $\delta^{13}\text{C}$  results were calibrated via linear regression against the international standards Air (as atmospheric dinitrogen with  $^{15}\text{N}:^{14}\text{N}$  ratio of 3.676 (Junk and Svec 1958)) and Vienna Pee Dee Belmite (VPDB; with  $^{13}\text{C}:^{12}\text{C}$  ratio of 0.011180 (Coplen 1995; Carter and Fry 2013)); respectively. Enriched  $\delta^{15}\text{N}$  values generally indicate pedogenically older soils that have a relatively greater developmental age with more established plant and microbial communities; also, they may indicate denitrification activity in the soil as part of a well-established N cycle or the rate of nitrogen cycling (Emmett et al. 1998; Bedard-Haughn et al. 2003; Huber et al. 2007; Binkley and Högberg 2016).

Soil texture was determined by hydrometer method (Kroetsch and Wang 2008), with measurements taken at the 40 s and 7 h intervals to accurately determine percent of sand, silt, and clay within the samples. Vegetation cover (%) and dominant species cover at each flux chamber was determined from visual inspection and analysis of photographs for the area around each chamber base of  $50 \times 50$  cm.

Additional composited soil samples ( $n = 12$ ) were also collected using ethanol sterilized tools and whirlpaks for phospholipid fatty acid (PLFA) analysis to determine the changes in microbial community at RDG and Alpine sites. These soil samples for microbial analyses were kept on ice in a cooler for less than 48 h total before being transferred to a  $-80$  °C freezer at the University of Alberta. Following extraction of the PLFA's, samples were analyzed identically to Kiani et al. (2017). An Agilent 6890 Series capillary gas chromatograph (Agilent Technologies, Wilmington, DE, USA) and MIDI peak identification software were used to identify the PLFA's in each sample. Peaks were classified as gram negative bacteria, gram positive bacteria, and fungi according to known PLFA's (Frostegard et al. 1996; Myers et al. 2001; Hamman et al. 2007).

#### Statistical analyses

The flux measurements for both  $\text{CH}_4$  and  $\text{CO}_2$  were subject to multiple comparisons between site types and times of measurements. T-tests were used to

compare between the RDG and Alpine sites and between the morning and afternoon measurements. One-way ANOVA was used to compare between days, elevational bands along the transects, and between individual chambers, after confirming normality with Kruskal–Wallis tests.

Potential mechanisms driving soil fluxes for both  $\text{CH}_4$  and  $\text{CO}_2$  were analyzed using regression trees and path analyses. The regression trees were constructed using both the *rpart* and *party* packages in R (Hothorn et al. 2006; Therneau et al. 2015; R Core Development Team 2017). Both packages use recursive partitioning to construct the trees, however *rpart* uses the Gini index to evaluate the splits in the data while *party* uses permutation tests to select variables. *rpart* and the Gini index have been criticized as often overfitting data, whereas *party* reduces overfitting with a p value criteria the splits must pass; however, it also forces the data to be evaluated by permutation significance tests that may not be appropriate for all data. Using multiple lines of evidence helps to reduce bias inherent in a single test (Munafò and Davey Smith 2018). The common variables selected by both regression tree tests will be the strongest explanatory variables for the flux data and focused on as the primary drivers. Variables selected by one method but not the other are more tenuous as potential drivers for explaining fluxes.

The recursive nature of regression trees allows them to identify complex relationships within the data, and they often perform better than logistic regression (Karels et al. 2004; Mitchell et al. 2009). Regression trees are non-parametric, and so do not make assumptions about data distribution and can accommodate incomplete datasets (De'ath and Fabricius 2000; Karels et al. 2004; Mitchell et al. 2009). Variables used in construction of the trees were all remaining variables after selection by variance inflation factors (VIF). Where the VIF's for all properties were determined the largest were removed and then all the properties checked again. This selection process continued iteratively until all remaining variables were found to have VIF's below 4 which removed all cases of multicollinearity between variables. The remaining variables were used to construct the regression trees. Since the variables were identical for both the  $\text{CH}_4$  and  $\text{CO}_2$  fluxes, as they were measured concurrently, the properties that remained for analysis were: soil temperature, soil moisture,

$\text{NO}_3^-$ , % clay, % vegetation cover, and primary vegetation (the species with the highest percentage cover at each site). Path analyses were constructed using the variables that were shown to be important by the regression trees using the lavaan package in R (Rosseel 2012).

## Results

### Influence of location and date on fluxes

The mean  $\text{CH}_4$  flux for all sites the study period was  $-58 \mu\text{g C m}^{-2} \text{h}^{-1}$ , the mean  $\text{CO}_2$  flux for all sites across the study period was  $48 \text{ mg C m}^{-2} \text{h}^{-1}$ .  $\text{CH}_4$  and  $\text{CO}_2$  fluxes were similar over 3 days of measurements ( $\text{CO}_2:\text{F}_{1,175} = 3.125$ ,  $p = 0.079$ ;  $\text{CH}_4:\text{F}_{1,175} = 0.126$ ,  $p = 0.723$ ) and there was no difference between the fluxes at different times of the day (morning or afternoon) for  $\text{CH}_4$  ( $t_{147,14} = -0.766$ ,  $p = 0.445$ ). However, there was an effect of time of day on  $\text{CO}_2$  measurements ( $t_{163,43} = 2.370$ ,  $p = 0.019$ ), with significantly stronger  $\text{CO}_2$  efflux occurring in the afternoon compared to morning for the RDG ( $t_{57,753} = -4.704$ ,  $p < 0.001$ ) and Alpine sites ( $t_{57,99} = -2.724$ ,  $p = 0.009$ ). However, for sites on the successional gradient, this effect was not significant ( $t_{15,706} = -0.317$ ,  $p = 0.756$ ).

The significant difference in methane fluxes between the RDG ( $5 \mu\text{g CH}_4\text{-C m}^{-2} \text{hr}^{-1}$ ) and Alpine ( $-112 \mu\text{g CH}_4\text{-C m}^{-2} \text{h}^{-1}$ ) sites ( $t_{59} = 10.19$ ,  $p < 0.001$ ) was due to RDG sites not having any measurable methane fluxes. Methane fluxes were also significantly different between the successional sites along the transects ( $F_{2,54} = 61.18$ ,  $p < 0.001$ ). A post hoc Tukey HSD test showed that low ( $1 \mu\text{g CH}_4\text{-C m}^{-2} \text{h}^{-1}$ ), mid ( $-155 \mu\text{g CH}_4\text{-C m}^{-2} \text{h}^{-1}$ ) and high ( $-33 \mu\text{g CH}_4\text{-C m}^{-2} \text{h}^{-1}$ ) sites were significantly different from each other, with mid sites having approximately four times greater methane uptake than the high site. A significant difference in the  $\text{CO}_2$  fluxes was also found between the RDG and Alpine sites ( $t_{61,035} = -14.733$ ,  $p < 0.001$ ). The mean  $\text{CO}_2$  efflux in the Alpine sites was over 18 times greater than in the RDG sites. The  $\text{CO}_2$  fluxes also differed along the successional transects, with the high elevation site having significantly lower  $\text{CO}_2$  emissions compared to the mid and low sites ( $F_{2,54} = 47.89$ ,  $p < 0.001$ ). A post hoc Tukey HSD test showed that all successional sites

were significantly different, with the high sites having the lowest  $\text{CO}_2$  efflux.

### Statistical linkages determined by regression trees

Two R packages (party and rpart) were used to construct regression trees, but differed in which variables were used to split both the  $\text{CH}_4$  and  $\text{CO}_2$  fluxes. The rpart regression tree for the entire methane dataset split the data by soil total carbon,  $\delta^{15}\text{N}$ , moisture, and % clay (Fig. 1a). This tree was less complicated than the party methane regression tree (Fig. 2a), but the two were primarily split by the same variables. The only difference in variables selected by the two methods was soil surface temperature selected by party, suggesting that TC,  $\delta^{15}\text{N}$ , and moisture are strong predictors for methane fluxes. Soils with higher total carbon, higher  $\delta^{15}\text{N}$  (more developed), and less moisture had the strongest methane uptake. However, some of the splits within the dataset were to partition out some of the small, non-significant fluxes that were measured. To determine the potential drivers of the non-zero fluxes only, a subset of the data was subjected to a separate regression tree analysis. In total there were 76 consistent ( $R^2 > 0.9$ ) methane fluxes measured, indicating that approximately 43% of the methane fluxes measured were strong uptakes. When analyzing this subset of strong methane fluxes, the significant fluxes were split by soil total carbon and moisture according to both methods (Figs. 1b, 2b), although rpart also included  $\delta^{15}\text{N}$ . The strongest methane uptake was found when total carbon was high, moisture was low, and  $\delta^{15}\text{N}$  was high. There is evidence that when moisture is greater than 0.21 water fraction by volume (w.f.v), high total carbon could limit reduction in methane uptake meaning with relatively high total carbon ( $> 6.0\%$ ) methane uptake may remain strong even with high soil moisture (Fig. 2b). Overall, methane uptake was strongest when total carbon was greater than 4% and soil moisture was lower than 0.21 w.f.v (i.e. 210 mL of water per 1 L of soil).

Total carbon and moisture are common between both subset regression trees and reinforce the importance of those factors in driving methane fluxes in alpine soils. The relationship between moisture and the non-zero methane fluxes differed between sites, with both Alpine sites and high elevation sites having the strongest negative relationships ( $R^2 = 0.494$ ,



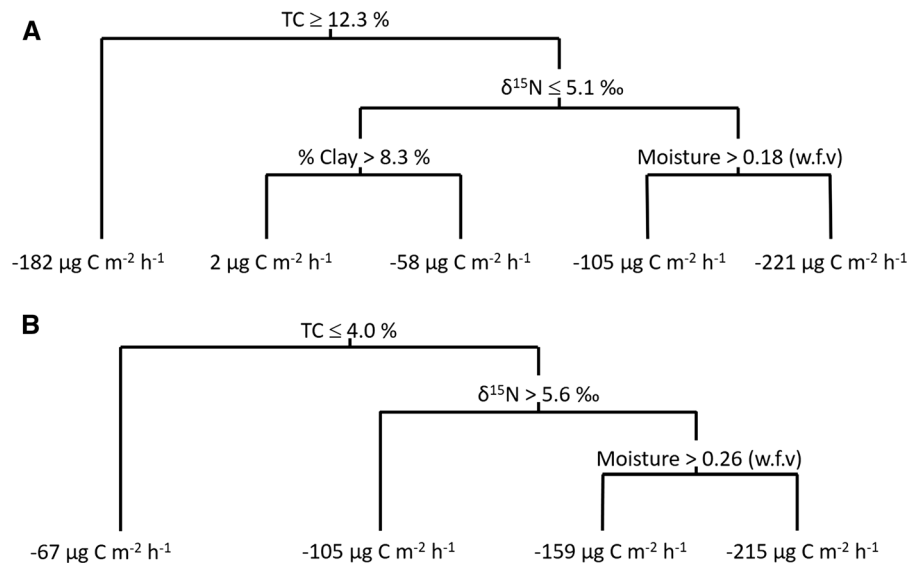


**Fig. 1** Regression trees determined using ‘rpart’ algorithm for methane fluxes. a The entire methane dataset showed that soils with total carbon (TC) greater than 12.3%,  $\delta^{15}\text{N}$  greater than 5, and moisture less than 0.18 w.f.v had the highest methane uptake. b The non-zero methane dataset indicated that sites with high TC, high  $\delta^{15}\text{N}$  and low moisture had the strongest methane

uptake. Nodes were split by recursive partitioning which attempts to split the data into smaller sets. When the condition of the node is met the data branches to the left. Each number under the node corresponds to the average methane uptake by the conditions for that node

$R^2 = 0.0939$ , and  $R^2 = 0.139$ ; respectively), but mid elevation sites showed a non-significant relationship ( $R^2 = 0.005$ ,  $R^2 = 0.010$ ; respectively; Fig. 3). Vegetation cover explained 27.6% of the variation in total methane fluxes (Fig. 3). The indirect effects of vegetation cover, such as carbon dynamics and moisture, likely drives methane uptake at Bachelor Pass.

The rpart regression tree for the  $\text{CO}_2$  fluxes split the data by % vegetation cover, % clay, soil temperature, and  $\delta^{15}\text{N}$  (Fig. 4). This tree was more simplified compared to the party regression tree for  $\text{CO}_2$ . The highest  $\text{CO}_2$  emissions were found in sites with high plant cover, high soil temperature, and  $\delta^{15}\text{N}$  enriched soils. The party regression tree analysis for the  $\text{CO}_2$  fluxes split the data by % vegetation cover twice, soil temperature twice, and moisture once (Fig. 5). The analysis shows that the  $\text{CO}_2$  fluxes were generally higher when the % vegetation cover was  $> 43\%$  (Fig. 5). Of those fluxes, those with warmer soil conditions tended to have stronger  $\text{CO}_2$  emissions.

Soil moisture, TC, and  $\delta^{15}\text{N}$  were selected as the explanatory variables in the path analysis for the entire methane dataset. There was a strong positive relationship between soil moisture and methane efflux

(meaning methane uptake declines in wetter soils), and a strong negative relationship between both soil total carbon and  $\delta^{15}\text{N}$  versus methane efflux (as total carbon or  $\delta^{15}\text{N}$  increases methane uptake also increases). The path analysis confirmed the relationships between total carbon and moisture on methane uptake. Overall, the path model explained two-thirds of the variance in methane fluxes based on goodness of fit ( $R^2 = 0.671$ ,  $p < 0.001$ ). For the subset methane dataset the variables used in the path analysis were: moisture, TC, and % vegetation cover. The strongest relationships were positive between moisture and methane efflux as well as negative between TC and methane efflux, similar to the entire dataset. The path model explained half of the variance in the significant methane fluxes ( $R^2 = 0.500$ ,  $p < 0.001$ ). The variables used in the path analysis for the  $\text{CO}_2$  fluxes were: soil temperature and % vegetation cover. % vegetation cover had the strongest (positive) relationship with  $\text{CO}_2$  emissions. Overall, the path model explained 69.4% of the variance in the  $\text{CO}_2$  fluxes ( $R^2 = 0.694$ ,  $p < 0.001$ ).

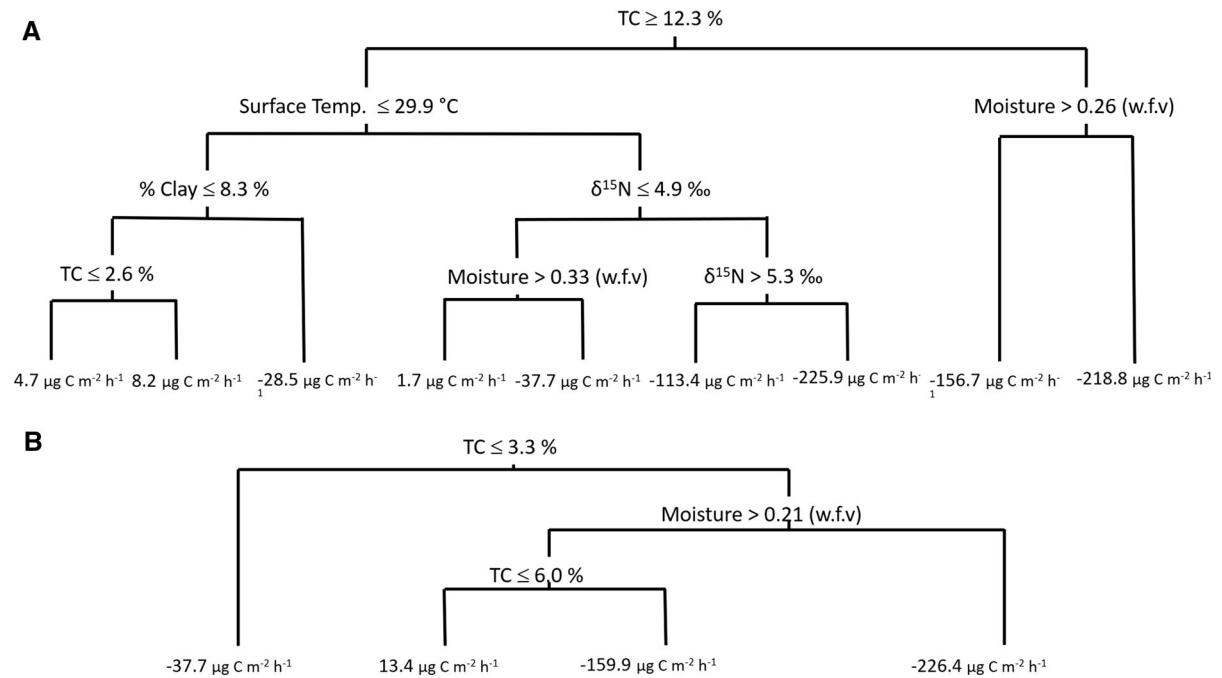


**Fig. 2** Regression trees determined using ‘party’ algorithm for methane fluxes **a** The entire methane dataset indicated that soils with TC greater than 12.3% and moisture less than 0.26 w.f.v had the highest methane uptake. **b** The non-zero methane dataset indicated that sites with high TC and low moisture had the strongest methane uptake. High total carbon ( $>$  6%) functioned

to reduce some of the loss of uptake experienced in moist conditions. The nodes were split by recursive partitioning which attempts to split the data into smaller sets. When the condition of the node is met the data branches to the left. Each number under the node corresponds to the median methane uptake predicted by the conditions for that node

## Discussion

Recently deglaciated soils did not uptake methane and contributed the least to  $\text{CO}_2$  emissions. These results were expected as both  $\text{CH}_4$  and  $\text{CO}_2$  fluxes are directly generated and also indirectly affected by microbial and vegetation communities which are largely absent in RDG sites (Table 2). Methane is primarily taken up by soils via methanotrophs, a group of microbes that oxidizes methane for energy (Hofmann et al. 2016b). The Alpine sites contained on average over two orders of magnitude greater numbers of PLFA’s in the soil than the RDG soils (Table 2). The observed increase in PLFA’s increases the likelihood that the more developed soils contain methanotrophs as part of an active microbial community, which will collectively enable the soil to uptake methane. Concomitantly, the low amount of PLFA’s in the RDG sites indicates that there is lower likelihood of these sites containing methanotrophs, which precludes soil methane uptake. PLFA data were not used in the regression tree analyses due to differences in sampling design,

however, microbial abundance is related to vegetation cover and total carbon as microbes require organic carbon sources as substrate (Esperschütz et al. 2011; Streit et al. 2014), which may account for our observation that total carbon was an important variable for splitting the data for both methane datasets (Fig. 1). The total carbon of the soil may act as a composite variable that contains and integrates influences from the plant and microbial communities. In addition to the microbial differences between the sites there is also a large difference in the % vegetation cover, where the RDG sites had at most 8% cover.  $\text{CO}_2$  release from soils is largely due to the cellular respiration occurring from the microbes and plant roots in the soil (Gulledge and Schimel 2000). Relative to RDG soils, the large microbial mass and plant cover present in the Alpine sites corresponds to much stronger  $\text{CO}_2$  effluxes.

The soil methane fluxes were mostly driven by soil TC and moisture, as well as  $\delta^{15}\text{N}$  and % clay by the two types of regression trees for both the entire and subset methane dataset. These variables encompass

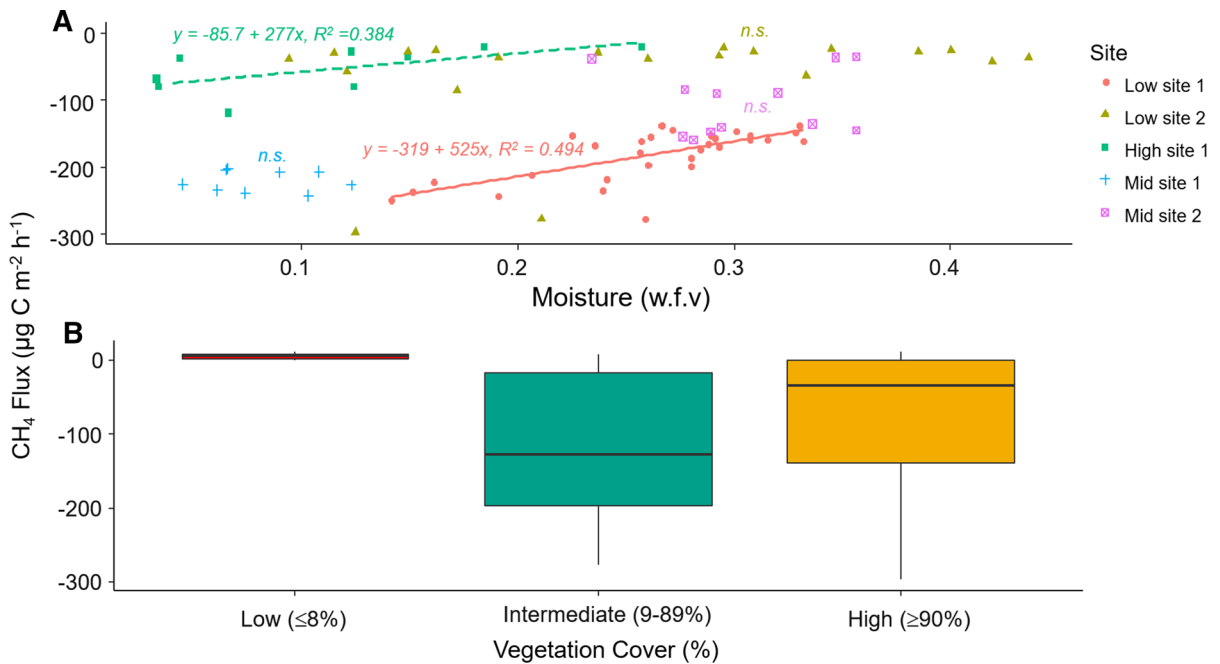


**Fig. 3** a Relationship between methane fluxes and soil volumetric water content indicating that lower moisture increases the strength of the methane uptake by soil at the low and high sites of transect 1. Other variables or complex interactions may drive the methane uptake at the other plotted sites, or more data could be needed. b Percentage vegetation

cover classes ( $n = 60$  for both the Low and Mid sites, and  $n = 57$  for the High site) indicating that vegetation cover between 9 and 89% (defined as intermediate range) generally corresponded to greater uptake of methane compared with high ( $\geq 90\%$ ) and low ( $\leq 8\%$ ) cover sites.

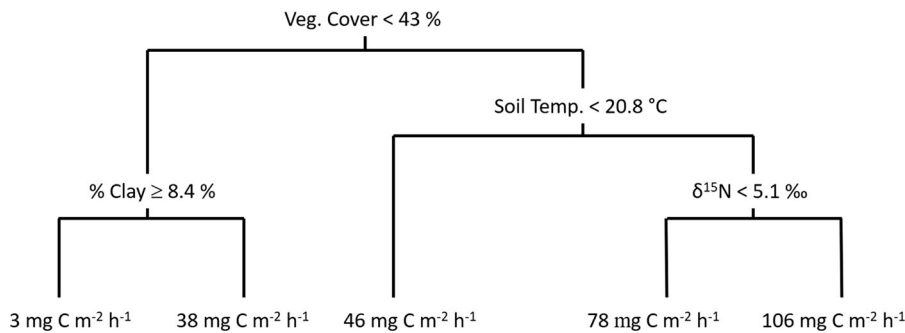


**Fig. 4** Regression tree determined using ‘rpart’ algorithm for  $\text{CO}_2$  fluxes High vegetation cover with high soil temperatures and  $\delta^{15}\text{N}$  contributed to the highest  $\text{CO}_2$  release from the soils. Low vegetation cover and more clay in the soil resulted in the lowest  $\text{CO}_2$  fluxes from the sites, which generally occurred in the recently deglaciated (RDG) sites. The nodes were split by

recursive partitioning which attempts to split the data into smaller sets so that it is easier to fit a regression to it. When the condition of the node is met the data splits to the left. Each number under the node corresponds to the average  $\text{CO}_2$  uptake by the conditions for that node

physico-chemical parameters that relate to potential soil microbial abundance (Hofmann et al. 2016b), and soil porosity. Carbon, soil development (as indicated through  $\delta^{15}\text{N}$ ), and moisture are all important for microbial communities. The net flux of methane is determined by the balance of methane production by

methanogens and methane consumption by methanotrophs. Hofmann et al. (2016b) found that methanogenic bacteria decreased with increasing altitude and were absent in the nival zone (similar to the recently deglaciated terrain in our study) on a mountain in Tyrol, Austria. Areas with higher plant cover and their

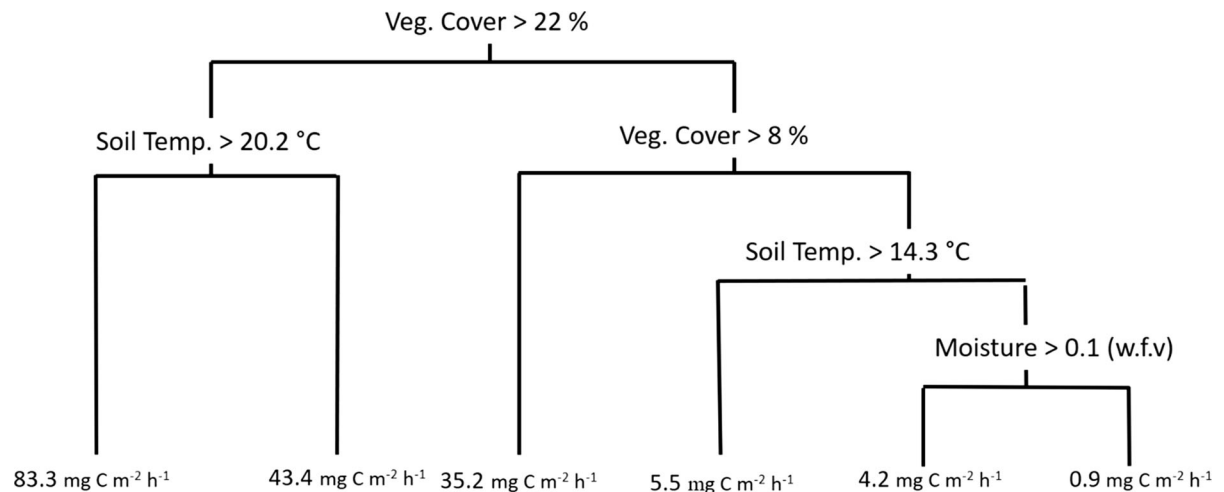


**Fig. 5** Regression trees determined using ‘party’ algorithm for CO<sub>2</sub> fluxes. High vegetation cover with high soil temperatures contributed to the highest CO<sub>2</sub> release from the soils. Extremely low vegetation cover, cooler temperatures and low moisture in the soil resulted in the lowest CO<sub>2</sub> fluxes, which generally occurred in the recently deglaciated (RDG) sites. The nodes

were split by recursive partitioning which attempts to split the data into smaller sets so that it is easier to fit a regression to it. When the condition of the node is met the data branches to the left. Each number under the node corresponds to the median CO<sub>2</sub> uptake predicted by the conditions for that node

**Table 2** Bacterial and fungal phospholipid fatty acids (PLFA) and the ratio of bacterial to fungal PLFA’s (Bac:Fun) for recently deglaciated (RDG) and Alpine sites.

Site	Gram– nmol g <sup>–1</sup>	Gram+ nmol g <sup>–1</sup>	Total bacteria nmol g <sup>–1</sup>	Fungi nmol g <sup>–1</sup>	Bac:Fun
RDG	6.6 ± 1.9	1.1 ± 0.6	7.8 ± 2.4	2.6 ± 0.6	2.8 ± 0.3
Alpine	435.2 ± 51.4	696.4 ± 85.0	1131.5 ± 135.9	329.3 ± 36.9	3.4 ± 0.1

Site refers to location from glacier terminus (Recently Deglaciated: RDG, and Alpine). Values are means (n = 6) ± 1 standard error (SE)

associated effects tended to have a higher abundance of methanogens, this likely holds for our study as well based on the PLFA’s from the RDG and Alpine sites. However, Hofmann et al. (2016b) found that methanotroph abundance did not seem to vary with altitude. We expected methane uptake in the RDG sites and declining uptake in the later successional areas. Instead we measured no uptake in the RDG sites and increasing methane uptake in areas with higher plant cover, larger soil total carbon concentration, and lower soil moisture. This pattern suggests that there was either an increase in the abundance and dominance of methanotrophs (or a decline in the number of methanogens) in the Alpine site, or that moisture conditions were more important for determining CH<sub>4</sub> uptake. Methane oxidation requires oxygen, if there is

high w.f.v neither atmospheric CH<sub>4</sub> nor oxygen will be able to find pathways for diffusion from the atmosphere into the soil, therefore, methane consumption by methanotrophs will be overwhelmed by methane production via methanogens. Likewise, upon oxidation of CH<sub>4</sub>, the resulting CO<sub>2</sub> would also need to be exchanged between the soil air and the atmosphere (Zhu et al. 2018). Fluctuations in soil water content affect both the microbial and physical drivers of methane fluxes regardless of soil and plant community development.

Soil total carbon was the primary driver of methane uptake identified by the regression trees (Fig. 1). Total carbon likely acts on methane fluxes by stimulating microbial activity and high carbon generally corresponds to higher microbial abundance and diversity

(Tscherko et al. 2004). Higher vegetation cover will lead to higher carbon accretion as plants release carbon compounds through litter production and their roots into the rhizosphere (Genxu et al. 2008). This indicates a synergistic linkage between increased vegetation cover and microbial activity to increase methane uptake. In addition to indirectly affecting the consumption of methane through the microbial community, vegetation can also influence fluxes indirectly through increased aeration of the soil either by removing moisture (plant water uptake) or by penetrating soil and developing soil structure through root growth and carbon additions. Changes in vegetation cover and associated soil properties will have a large effect on methane fluxes in the future.

Moisture was a consistent predictor of methane uptake in our soils, in particular when the vegetation cover was similar among sites. Soil moisture may be a key driver of vegetation abundance and indirectly soil carbon content, however, since methane uptake was highest in soils under dry or intermediate moisture conditions, it is likely through the regulation of aeration in the soil pores that moisture availability primarily drives methane fluxes. The influence of moisture on methane uptake in montane and alpine soils has been previously identified in both China, the USA and Switzerland (Torn and Harte 1996; Lazzaro et al. 2012; Chiri et al. 2015, 2017; Wei et al. 2015). Our results also support this relationship in the North Selkirk Mountains, suggesting moisture dependence is a widespread factor controlling methane feedback in mountain ecosystems.

Soil clay percentage was another physical driver of methane fluxes identified in our study. Soils with lower clay content had higher methane uptake. The low % clay can imply that soils with more sand and silt, and therefore larger pore space on average, are likely to have higher uptake of methane, possibly due to the ease of movement for gases in large, well connected pore spaces. In addition, soils enriched in clay typically retain more moisture (~ less aeration) over longer periods due to the high surface area of particles and dominance of small pores. However, soils with high sand content are likely also a detrimental extreme as they can be poor growing media for vegetation establishment and organic matter accrual, collectively leading to an overall lower methane uptake in such coarse-textured soils.

The soil CO<sub>2</sub> fluxes were primarily driven by vegetation cover, but are also impacted by % clay, δ<sup>15</sup>N, and soil temperature according to our results. Higher vegetation cover generally corresponds to higher microbial biomass as rhizospheres hold more microbial biomass than bulk soil (Berg and Smalla 2009). Microbes and plant roots both respire which increases the total amount of CO<sub>2</sub> released from the soil. Temperature also influenced the CO<sub>2</sub> emissions which are mediated by plant and microbial abundance, rate of enzymatic reactions, and through physical effects on gas movement and diffusivity.

We did not observe an effect of time of day on the CO<sub>2</sub> fluxes from the Alpine or transect sites. The soil at the Alpine sites had a higher thermal buffer than the recently deglaciated sites, meaning that the soil temperature varied less over the day in more developed soils. The difference in diurnal temperature variation between sites could explain why time of day only affected the CO<sub>2</sub> fluxes at the RDG sites. Variability in soil temperatures across sites may be another reason for why soil temperature was a stronger predictor than air temperature for CO<sub>2</sub> emissions in our study. Measuring multiple temperatures (i.e. soil, surface, and air temperature) is advantageous for finding the most effective determinant of the CO<sub>2</sub> fluxes at a site as the best predictor may vary between ecosystems and soil types. The difference in soil daily average, maximum, and minimum temperature at the soil surface and belowground between similar field sites differing in elevation indicated qualitatively that belowground minimum temperatures may be the most important for upkeeping the differences in soil temperature at different elevations. Soil moisture was not found to be a strong determinant of CO<sub>2</sub> emissions despite previous research suggesting it is a primary driver (Borken et al. 2003; Parkin and Kaspar 2003).

We did not measure the CO<sub>2</sub> taken up by plants via photosynthesis. The uptake of CO<sub>2</sub> into the plant tissues could counterbalance emissions, effectively leading to ecosystem C accumulation by a gradual build-up of soil organic matter during succession. Although these processes occur over long periods, an evaluation of all C pools and fluxes in alpine environments as a function of succession and altitudinal gradients would be valuable.

## Comparison of methane fluxes across biomes

The methane uptake observed in our study is comparable to previous studies on alpine grassland methane fluxes where precipitation was found to limit methane uptake (Wei et al. 2015; Chiri et al. 2017; Fu et al. 2018). Methane uptake peaked during the growing season in China and declined (though there was still an uptake) during the wet season (Fu et al. 2018). Older soils along glacier forefields had stronger uptake of methane than did recently deglaciated (< 15 years) areas in Switzerland (Chiri et al. 2015, 2017; Rime et al. 2015; Zhu et al. 2018). This is consistent with our comparison between sites of different times since deglaciation, however we did not find significant uptake in the recently deglaciated sites. The average methane uptake rate quantified in our study was more intense and consistent than reported from previous studies in alpine regions (Wei et al. 2015; Chiri et al. 2017; Fu et al. 2018). Our alpine sites had an average methane uptake of approximately  $-112 \pm 12 \mu\text{g CH}_4\text{-C m}^{-2} \text{h}^{-1}$ , which is a higher rate of methane uptake compared to the values reported in the Tibetan Plateau (max uptake:  $-96 \mu\text{g CH}_4 \text{m}^{-2} \text{h}^{-1}$ ) (Wei et al. 2015).

Upscaling the methane uptake at our study site to all alpine areas (3% of Earth surface, Nagy and Grabherr 2009), would account for approximately  $-3.8 \pm 0.4 \text{Tg CH}_4\text{-C year}^{-1}$  from the atmosphere. This value is certainly an overestimation of the total uptake contribution of alpine regions to the global methane budget, and does not account for the seasonality of fluxes in these environments. Variability of methane fluxes in alpine environments are largely uncharacterized (Murguía-Flores et al. 2018), but have been recognized as potentially significant in the 2019 IPCC Special Report on Oceans and the Cryosphere (IPCC 2019). The estimation of global methane uptake for all aggregated terrestrial surface suggests a sink of  $-22 \pm 12 \text{Tg CH}_4 \text{year}^{-1}$  based on an area-weighted stratification by climatic zone, ecosystem type, and soil texture (Dutaur and Verchot 2007).

The uptake of methane in alpine areas is comparable to that of low elevation temperate grassland habitat, which also shows a net methane uptake (Mosier et al. 1991; Praeg et al. 2017). Temperature was a key driver of methane uptake in temperate grasslands, with the strongest uptake occurring at warmer temperatures. High temperatures can increase

methane uptake in grassland soils above that of upland forest soils (Praeg et al. 2017), generally considered to be the strongest sinks of atmospheric methane.

Climate change is predicted to advance treeline upslope into alpine regions which will affect the current vegetation composition and the strength of methane fluxes from the soil (Gottfried et al. 2012; Bourgeron et al. 2015; Lamprecht et al. 2018). Current temperate upland forests account for a large proportion of the estimated methane captured from the atmosphere globally; roughly 4–10% of global methane sinks (Dutaur and Verchot 2007; Pitz and Megonigal 2017). There was also some methane consumption found in lowland forest soils, though it was weaker and less consistent than the upland forest (Gulledge and Schimel 2000). The contribution of methane emitted throughout plant transpiration from the soil water into the atmosphere requires additional measurements to better constraint these values (Keppler et al. 2006; Nisbet et al. 2009; Pitz and Megonigal 2017). Future altitudinal treeline advance may result in the alpine zone becoming an even stronger sink for methane compared with lower elevation grassland and forest soils.

Arctic tundra is generally considered to be a small sink for methane, depending on site moisture (King et al. 1998; Reeburgh et al. 1998; Nauta et al. 2015; Voigt et al. 2017; St. Pierre et al. 2019). With increasing shrub expansion and drying soils, it may become an even greater sink (Myers-Smith et al. 2011). However, Zona et al. (2016) reported that overall the Arctic may be a net source of methane, in particular in the cold season due to emissions occurring in the thawed active layer that may persist for a long time under a thick snowpack. Zona et al. (2016) also measured fluxes across a range of sites that included dry tundra (methane sink) and tundra bogs and fens (methane source). At this scale Zona et al. (2016) found that the source of methane from peatlands outweighs the sinks from dry upland sites.

Comparatively, methane emissions from peatlands globally account for approximately 20% of all natural emissions (Olefeldt et al. 2017). The effluxes from peatland systems are generally higher than the methane sinks we observed at our study site (Pelletier et al. 2007; Olefeldt et al. 2017). Therefore, the global methane budget, even including alpine habitat, tends to suggest methane addition to the atmosphere from terrestrial ecosystems. However, with glacial



recession and treeline advance upslope, the alpine is likely to experience a net surface expansion, and hence likely become a greater sink over time, whereas with increasing ambient temperatures, many peatlands are starting to drain and dry which leads to a weakening in their methane emissions (Minke et al. 2016; Olefeldt et al. 2017). It will be useful to continue to quantify the potential contribution of methane consumption by alpine landscapes with ongoing climate change.

**Acknowledgements** We are grateful for the assistance of Rüdiger Kaufmann, Lorelies Ortner, and Felicity Hik in the field, and Allan Harms, Brett Feland, and Jela Burkas in the laboratory. We acknowledge support from the Natural Sciences and Engineering Research Council Canada (Discovery Grant RGPIN-06691 to DSH), the Canada Foundation for Innovation, Departments of Biological Sciences and Renewable Resources at the University of Alberta, and The Alpine Club of Canada.

#### Compliance with ethical standards

**Conflict of interest** The authors declare that they have no conflict of interest.

#### References

- Bedard-Haughn A, Van Groenigen JW, Van Kessel C (2003) Tracing  $^{15}\text{N}$  through landscapes: potential uses and precautions. *J Hydrol* 272:175–190. [https://doi.org/10.1016/S0022-1694\(02\)00263-9](https://doi.org/10.1016/S0022-1694(02)00263-9)
- Berg G, Smalla K (2009) Plant species and soil type cooperatively shape the structure and function of microbial communities in the rhizosphere. *FEMS Microbiol Ecol* 68:1–13. <https://doi.org/10.1111/j.1574-6941.2009.00654.x>
- Binkley D, Högberg P (2016) Tamm review: revisiting the influence of nitrogen deposition on Swedish forests. *For Ecol Manag* 368:222–239. <https://doi.org/10.1016/j.foreco.2016.02.035>
- Borken W, Davidson EA, Savage K et al (2003) Drying and wetting effects on carbon dioxide release from organic horizons. *Soil Sci Soc Am J* 67:1888. <https://doi.org/10.2136/sssaj2003.1888>
- Bourgeron PS, Humphries HC, Liptzin D, Seastedt TR (2015) The forest–alpine ecotone: a multi-scale approach to spatial and temporal dynamics of treeline change at Niwot Ridge. *Plant Ecol Divers* 8:763–779. <https://doi.org/10.1080/17550874.2015.1126368>
- Brachmann CG (2019) Characteristics of alpine plants and soils along an elevational gradient, Northern Selkirk Mountains, British Columbia (MSc Thesis). University of Alberta
- Brooks PD, Schmidt SK, Williams MW (1997) Winter production of  $\text{CO}_2$  and  $\text{N}_2\text{O}$  from alpine tundra: Environmental controls and relationship to inter-system C and N fluxes. *Oecologia* 110:403–413. <https://doi.org/10.1007/PL00008814>
- Camarero JJ, Linares JC, García-Cervigón AI et al (2017) Back to the future: the responses of alpine treelines to climate warming are constrained by the current ecotone structure. *Ecosystems* 20:683–700. <https://doi.org/10.1007/s10021-016-0046-3>
- Cannone N, Pignatti S (2014) Ecological responses of plant species and communities to climate warming: upward shift or range filling processes? *Clim Chang* 123:201–214. <https://doi.org/10.1007/s10584-014-1065-8>
- Carter JF, Fry B (2013) “Do it yourself” reference materials for  $\Delta^{13}\text{C}$  determinations by isotope ratio mass spectrometry. *Anal Bioanal Chem* 405:4959–4962. <https://doi.org/10.1007/s00216-013-6851-z>
- Chersich S, Rejšek K, Vranová V et al (2015) Climate change impacts on the Alpine ecosystem: an overview with focus on the soil—a review. *J For Sci* 61:496–514. <https://doi.org/10.17221/47/2015-JFS>
- Chikowo R, Mapfumo P, Nyamugafata P, Giller KE (2004) Mineral N dynamics, leaching and nitrous oxide losses under maize following two-year improved fallows on a sandy loam soil in Zimbabwe. *Plant Soil* 259:315–330. <https://doi.org/10.1023/B:PLSO.0000020977.28048.f0>
- Chiri E, Nauer PA, Henneberger R et al (2015) Soil-methane sink increases with soil age in forefields of alpine glaciers. *Soil Biol Biochem* 84:83–95. <https://doi.org/10.1016/j.soilbio.2015.02.003>
- Chiri E, Nauer PA, Rainer E-M et al (2017) High temporal and spatial variability of atmospheric-methane oxidation in Alpine glacier-forefield soils. *Appl Environ Microbiol* 83:AEM.01139–A17. <https://doi.org/10.1128/AEM.01139-17>
- Coplen TB (1995) Reporting of stable carbon, hydrogen, and oxygen isotopic abundances. *Ref Intercomp Mater stable Isot Light Elem - IAEA-TECDOC* 825:31–34
- Davis EL, Hager HA, Gedalof Z (2018) Soil properties as constraints to seedling regeneration beyond alpine treelines in the Canadian Rocky Mountains. *Arct Antarct Alp Res* 50:1–15. <https://doi.org/10.1080/15230430.2017.1415625>
- De'ath G, Fabricius KE (2000) Classification and regression trees: a powerful yet simple technique for ecological data analysis. *Ecology* 81:3178–3192
- Dutaur L, Verchot LV (2007) A global inventory of the soil  $\text{CH}_4$  sink. *Global Biogeochem Cycles* 21:1–9. <https://doi.org/10.1029/2006GB002734>
- Emmett BA, Kjønaas OJ, Gundersen P et al (1998) Natural abundance of  $^{15}\text{N}$  in forests across a nitrogen deposition gradient. *For Ecol Manag* 101:9–18
- Esperschütz J, Pérez-De-Mora A, Schreiner K et al (2011) Microbial food web dynamics along a soil chronosequence of a glacier forefield. *Biogeosciences* 8:3283–3294. <https://doi.org/10.5194/bg-8-3283-2011>
- Frostegård A, Baath E, Frostegård Å, Bååth E (1996) The use of phospholipid fatty acid analysis to estimate bacterial and fungal biomass in soil. *Biol Fertil Soils* 22:59–65. <https://doi.org/10.1007/BF00384433>
- Fu Y, Liu C, Lin F et al (2018) Quantification of year-round methane and nitrous oxide fluxes in a typical alpine shrub meadow on the Qinghai-Tibetan Plateau. *Agric Ecosyst*

- Environ 255:27–36. <https://doi.org/10.1016/j.agee.2017.12.003>
- Genxu W, Yuanshou L, Yibo W, Qingbo W (2008) Effects of permafrost thawing on vegetation and soil carbon pool losses on the Qinghai-Tibet Plateau, China. *Geoderma* 143:143–152. <https://doi.org/10.1016/j.geoderma.2007.10.023>
- Gottfried M, Pauli H, Futschik A et al (2012) Continent-wide response of mountain vegetation to climate change. *Nat Clim Chang* 2:111–115. <https://doi.org/10.1038/nclimate1329>
- Gulledge J, Schimel JP (2000) Controls on soil carbon dioxide and methane fluxes in a variety of taiga forest stands in interior Alaska. *Ecosystems* 3:269–282. <https://doi.org/10.1007/s100210000025>
- Hamman ST, Burke IC, Stromberger ME (2007) Relationships between microbial community structure and soil environmental conditions in a recently burned system. *Soil Biol Biochem* 39:1703–1711. <https://doi.org/10.1016/j.soilbio.2007.01.018>
- Hofmann K, Farbmacher S, Illmer P (2016a) Methane flux in montane and subalpine soils of the Central and Northern Alps. *Geoderma* 281:83–89. <https://doi.org/10.1016/j.geoderma.2016.06.030>
- Hofmann K, Pauli H, Praeg N et al (2016b) Methane-cycling microorganisms in soils of a high-alpine altitudinal gradient. *FEMS Microbiol Ecol* 92:1–10. <https://doi.org/10.1093/femsec/fiw009>
- Hothorn T, Hornik K, Zeileis A (2006) Unbiased recursive partitioning: a conditional inference framework. *J Comput Graph Stat* 15:651–674
- Hu FS, Bliss LC (2018) Tundra. *Encycl. Britannica*
- Huber E, Wanek W, Gottfried M et al (2007) Shift in soil-plant nitrogen dynamics of an alpine-nival ecotone. *Plant Soil* 301:65–76. <https://doi.org/10.1007/s11104-007-9422-2>
- IPCC (2019) IPCC special report on the ocean and cryosphere in a changing climate. In: Pörtner H-O, Roberts DC, Masson-Delmotte V, Zhai P, Tignor M, Poloczanska E, Mintenbeck K, Alegría A, Nicolai M, Okem A, Petzold J, Rama B, Weyer NM (eds). (in press)
- Junk G, Svec HJ (1958) The absolute abundance of the nitrogen isotopes in the atmosphere and compressed gas from various sources. *Geochim Cosmochim Acta* 14:234–243
- Karels TJ, Bryant AA, Hik DS (2004) Comparison of discriminant function and classification tree analyses for age classification of marmots. *Oikos* 105:575–587. <https://doi.org/10.1111/j.0030-1299.2004.12732.x>
- Keppler F, Hamilton JTG, Braß M, Röckmann T (2006) Methane emissions from terrestrial plants under aerobic conditions. *Nature* 439:187–191. <https://doi.org/10.1038/nature04420>
- Kiani M, Hernandez-Ramirez G, Quideau S et al (2017) Quantifying sensitive soil quality indicators across contrasting long-term land management systems: crop rotations and nutrient regimes. *Agric Ecosyst Environ* 248:123–135. <https://doi.org/10.1016/j.agee.2017.07.018>
- King JY, Reeburgh WS, Regli SK (1998) Methane emission and transport by arctic sedges in Alaska: results of a vegetation removal experiment. *J Geophys Res Atmos* 103:29083–29092. <https://doi.org/10.1029/98JD00052>
- Kitzler B, Zechmeister-Boltenstern S, Holtermann C et al (2006) Controls over N<sub>2</sub>O, NO<sub>x</sub> and CO<sub>2</sub> fluxes in a calcareous mountain forest soil. *Biogeosci Discuss* 2:1423–1455. <https://doi.org/10.5194/bg-3-383-2006>
- Knowles JF, Burns SP, Blanken PD, Monson RK (2015) Fluxes of energy, water, and carbon dioxide from mountain ecosystems at Niwot Ridge, Colorado. *Plant Ecol Divers* 8:663–676. <https://doi.org/10.1080/17550874.2014.904950>
- Koch O, Tschirko D, Kandeler E (2007) Seasonal and diurnal net methane emissions from organic soils of the Eastern Alps, Austria: effects of soil temperature, water balance, and plant biomass. *Arct Antarct Alp Res* 39:438–448. [https://doi.org/10.1657/1523-0430\(06-020](https://doi.org/10.1657/1523-0430(06-020)
- Kroetsch D, Wang C (2008) Chap. 55: particle size distribution
- Lamprecht A, Semenchuk PR, Steinbauer K et al (2018) Climate change leads to accelerated transformation of high-elevation vegetation in the central Alps. *New Phytol*. <https://doi.org/10.1111/nph.15290>
- Lazzaro A, Brankatschk R, Zeyer J (2012) Seasonal dynamics of nutrients and bacterial communities in unvegetated alpine glacier forefields. *Appl Soil Ecol* 53:10–22. <https://doi.org/10.1016/j.apsoil.2011.10.013>
- Lin JC, Mallia DV, Wu D, Stephens BB (2017) How can mountaintop CO<sub>2</sub> observations be used to constrain regional carbon fluxes? *Atmos Chem Phys* 17:5561–5581. <https://doi.org/10.5194/acp-17-5561-2017>
- Minke M, Augustin J, Burlo A et al (2016) Water level, vegetation composition, and plant productivity explain greenhouse gas fluxes in temperate cutover fens after inundation. *Biogeosciences* 13:3945–3970. <https://doi.org/10.5194/bg-13-3945-2016>
- Mitchell MG, Cahill JF, Hik DS (2009) Plant interactions are unimportant in a subarctic-alpine plant community. *Ecology* 90:2360–2367
- Mosier A, Schimel D, Valentine D et al (1991) Methane and nitrous oxide fluxes in native, fertilized and cultivated grasslands. *Nature* 350:330–332
- Munafò MR, Davey Smith G (2018) Repeating experiments is not enough. *Nature* 553:399–401. <https://doi.org/10.1038/d41586-018-01023-3>
- Murguía-Flores F, Arndt S, Ganesan AL et al (2018) Soil Methanotrophy Model (MeMo v1.0): a process-based model to quantify global uptake of atmospheric methane by soil. *Geosci Model Dev* 11:2009–2032. <https://doi.org/10.5194/gmd-11-2009-2018>
- Mutschlechner M, Praeg N, Illmer P (2018) The influence of cattle grazing on methane fluxes and engaged microbial communities in alpine forest soils. *FEMS Microbiol Ecol* 94:1–11. <https://doi.org/10.1093/femsec/fiy019>
- Myers RT, Zak DR, White DC, Peacock A (2001) Landscape-level patterns of microbial community composition and substrate use in upland forest ecosystems. *Soil Sci Soc Am J* 65:359–367
- Myers-Smith IH, Forbes BC, Wilmking M et al (2011) Shrub expansion in tundra ecosystems: dynamics, impacts and research priorities. *Environ Res Lett* 6:1–15. <https://doi.org/10.1088/1748-9326/6/4/045509>
- Nagy L, Grabherr G (2009) The biology of alpine habitats. Oxford University Press, Oxford

- Nauta AL, Heijmans MMPD, Blok D et al (2015) Permafrost collapse after shrub removal shifts tundra ecosystem to a methane source. *Nat Clim Chang* 5:67–70. <https://doi.org/10.1038/nclimate2446>
- Neu V, Neill C, Krusche AV (2011) Gaseous and fluvial carbon export from an Amazon forest watershed. *Biogeochemistry* 105:133–147. <https://doi.org/10.1007/s10533-011-9581-3>
- Nisbet RE, Fisher R, Nimmo R et al (2009) Emission of methane from plants. *Proc R Soc B Biol Sci* 276:1347–1354. <https://doi.org/10.1098/rspb.2008.1731>
- Oertel C, Matschullat J, Zurba K et al (2016) Greenhouse gas emissions from soils—a review. *Chem Erde* 76:327–352. <https://doi.org/10.1016/j.chemer.2016.04.002>
- Olefeldt D, Euskirchen ES, Harden J et al (2017) A decade of boreal rich fen greenhouse gas fluxes in response to natural and experimental water table variability. *Glob Chang Biol* 23:2428–2440. <https://doi.org/10.1111/gcb.13612>
- Parkin TB, Kaspar TC (2003) Temperature controls on diurnal carbon dioxide flux. *Soil Sci Soc Am J* 67:1763. <https://doi.org/10.2136/sssaj2003.1763>
- Pelletier L, Moore TR, Roulet NT et al (2007) Methane fluxes from three peatlands in the La Grande Rivière watershed, James Bay lowland, Canada. *J Geophys Res Biogeosci* 112:1–12. <https://doi.org/10.1029/2006JG000216>
- Pepin N, Bradley RS, Diaz HF et al (2015) Elevation-dependent warming in mountain regions of the world. *Nat Clim Chang* 5:424–430. <https://doi.org/10.1038/nclimate2563>
- Pitz S, Megonigal JP (2017) Temperate forest methane sink diminished by tree emissions. *New Phytol* 214:1432–1439. <https://doi.org/10.1111/nph.14559>
- Praeg N, Wagner AO, Illmer P (2017) Plant species, temperature, and bedrock affect net methane flux out of grassland and forest soils. *Plant Soil* 410:193–206. <https://doi.org/10.1007/s11104-016-2993-z>
- R Core Development Team (2017) R: a language and environment for statistical computing
- Reeburgh WS, King JY, Regli SK et al (1998) A CH<sub>4</sub> emission estimate for the Kuparuk River basin, Alaska. *J Geophys Res* 103:5–13
- Rime T, Hartmann M, Brunner I et al (2015) Vertical distribution of the soil microbiota along a successional gradient in a glacier forefield. *Mol Ecol* 24:1091–1108. <https://doi.org/10.1111/mec.13051>
- Rosseel Y (2012) lavaan: an R package for structural equation modeling. *J Stat Softw* 48:1–36
- Simony PS, Carr SD (2011) Cretaceous to Eocene evolution of the southeastern Canadian Cordillera: Continuity of Rocky Mountain thrust systems with zones of “in-sequence” mid-crustal flow. *J Struct Geol* 33:1417–1434. <https://doi.org/10.1016/j.jsg.2011.06.001>
- Smith K, Ball T, Conen F et al (2003) Exchange of greenhouse gases between soil and atmosphere: interactions of soil physical factors and biological processes. *Eur J Soil Sci* 54:779–791. <https://doi.org/10.1046/j.1365-2389.2003.00567.x>
- St. Pierre KA, Danielson BK, Hermesdorf L et al (2019) Drivers of net methane uptake across Greenlandic dry heath tundra landscapes. *Soil Biol Biochem*. <https://doi.org/10.1016/j.soilbio.2019.107605>
- Streit K, Hagedorn F, Hiltbrunner D et al (2014) Soil warming alters microbial substrate use in alpine soils. *Glob Chang Biol* 20:1327–1338. <https://doi.org/10.1111/gcb.12396>
- Therneau T, Atkinson B, Ripley B (2015) rpart: recursive partitioning and regression trees
- Torn MS, Harte J (1996) Methane consumption by montane soils: implications for positive and negative feedback with climatic change. *Biogeochemistry* 32:53–67
- Tscherko D, Hammesfahr U, Marx MC, Kandeler E (2004) Shifts in rhizosphere microbial communities and enzyme activity of *Poa alpina* across an alpine chronosequence. *Soil Biol Biochem* 36:1685–1698. <https://doi.org/10.1016/j.soilbio.2004.07.004>
- Venterea RT, Baker JM (2008) Effects of soil physical nonuniformity on chamber-based gas flux estimates. *Soil Sci Soc Am J* 72:1410. <https://doi.org/10.2136/sssaj2008.0019>
- Voigt C, Lamprecht RE, Marushchak ME et al (2017) Warming of subarctic tundra increases emissions of all three important greenhouse gases—carbon dioxide, methane, and nitrous oxide. *Glob Chang Biol* 23:3121–3138. <https://doi.org/10.1111/gcb.13563>
- Wei D, Ri X, Tarchen T et al (2015) Considerable methane uptake by alpine grasslands despite the cold climate: In situ measurements on the central Tibetan Plateau, 2008–2013. *Glob Chang Biol* 21:777–788. <https://doi.org/10.1111/gcb.12690>
- Wu L, Yang Y, Wang S et al (2017) Alpine soil carbon is vulnerable to rapid microbial decomposition under climate cooling. *ISME J* 11:2102–2111. <https://doi.org/10.1038/ismej.2017.75>
- Zhu X, Luo C, Wang S et al (2015) Effects of warming, grazing/cutting and nitrogen fertilization on greenhouse gas fluxes during growing seasons in an alpine meadow on the Tibetan Plateau. *Agric For Meteorol* 214–215:506–514. <https://doi.org/10.1016/j.agrformet.2015.09.008>
- Zhu B, Henneberger R, Weissert H et al (2018) Occurrence and origin of methane entrapped in sediments and rocks of a calcareous, Alpine glacial catchment. *J Geophys Res Biogeosci* 123:3633–3648. <https://doi.org/10.1029/2018JG004651>
- Zona D, Gioli B, Commane R et al (2016) Cold season emissions dominate the Arctic tundra methane budget. *Proc Natl Acad Sci* 113:40–45. <https://doi.org/10.1073/pnas.1516017113>

**Publisher's Note** Springer Nature remains neutral with regard to jurisdictional claims in published maps and institutional affiliations.